

# SPITE: Simple Polyhedral Intersection Techniques for modified Environments

Stav Ashur, Maria Lusardi\*, Marta Markowicz\*, James Motes, Marco Morales, Sariel Har-Peled, and Nancy M. Amato

Department of Computer Science, University of Illinois, 201 N. Goodwin Avenue,  
Urbana, IL 61801, USA

**Abstract.** Motion planning in modified environments is a challenging task, as it compounds the innate difficulty of the motion planning problem with a changing environment. This renders some algorithmic methods such as probabilistic roadmaps less viable, as nodes and edges may become invalid as a result of these changes. In this paper, we present a method of transforming any configuration space graph, such as a roadmap, to a dynamic data structure capable of updating the validity of its nodes and edges in response to discrete changes in obstacle positions. We use methods from computational geometry to compute 3D swept volume approximations of configuration space points and curves to achieve 10-40 percent faster updates and up to 60 percent faster motion planning queries than previous algorithms while requiring a significantly shorter pre-processing phase, requiring minutes instead of hours needed by the competing method to achieve somewhat similar update times.

## 1 Introduction

In the motion planning problem, we are given a robot  $r$  and an environment  $E = \{B, O\}$  (aka *workspace*) which is composed of a bounding box  $B$ , a set of obstacles  $O$ , and two configurations  $s$  and  $t$  of  $r$  in  $E$ , and we are tasked with deciding whether there exists a valid, i.e. collision free, sequence of movements taking  $r$  from configuration  $s$  to  $t$ .

A common approach in designing motion planning algorithms is to reduce the problem to finding a curve in the space of valid configurations, a subset of the implicitly defined *configuration space* (*C-space*) [14] of  $r$ , with the points corresponding to configurations  $s$  and  $t$  as its endpoints. These algorithms often build a geometric graph in the *C-space* called a *roadmap* whose nodes and edges represent feasible configurations and valid continuous motions of  $r$  in  $E$  respectively [11]. These representations often assume an environment in which obstacle positions never change.

In this paper, we tackle the problem of enhancing such roadmaps to account for the possibility of discrete changes in the obstacles' positions. These changes occur in multi-agent task and motion planning problems (i.e., multi-robot and

---

\*Equal contribution



Fig. 1: An image of the 5DOF UR5e robot used in physical experiments to test the validity of paths produced in simulation. Shelf environments are likely to be modified as stored items are added, removed, or placed in new locations.

human-robot collaborations), where agents can move objects, or in methods which seek to re-utilize plans generated earlier. See Figure 2 for an illustration.

The main challenge is to update the validity of nodes and edges in the roadmap (corresponding to points and curves in  $C$ -space) given changes in the workspace, as the effects of such changes on the  $C$ -space are not well understood. Intuitively, by continuity, small changes in object positions should result in local effects in the roadmap, as it is a geometric graph. Thus, one can hope that a relatively efficient graph data structure can help with this task.

**Contribution** We present a supplemental algorithm for roadmaps that can quickly find the set of nodes and edges whose validity status was altered due to a change in the workspace. While our contribution is not a motion planning algorithm, it is designed for multi query motion planning scenarios and enables quick computation of motion planning queries in a single environment for a known robot. Any graph-based SBMP algorithm can be paired with our method in order to generate an augmented roadmap that can maintain its functionality in the presence of workspace changes using less pre-processing time and faster updates than the previously best known method.

We achieve this improvement with a second contribution, an approach to 3D workspace volume approximations which enables us to store approximated robot configurations and swept volumes in a  $kD$ -tree like data structure which we use for fast hierarchical collision checking. This enables us to obtain a set of nodes and edges which may be affected by some modification made to the environment, and either invalidate or re-validate them.

**Evaluation** We compare our method with what is, to the best of our knowledge, the only method that produces a dynamic roadmap capable of updates in the

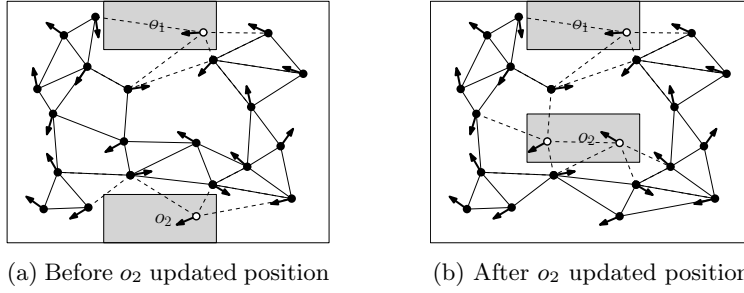


Fig. 2: A modified environment  $E = \{B, \{o_1, o_2\}\}$  with an overlaid roadmap for a small robot with two translational DOFs and one rotational DOF. The valid and invalid nodes of the graph are depicted as configurations with black and white centered points respectively, and valid and invalid edges are depicted as full and dashed segments respectively. The obstacle  $o_2$  moves from its first position seen in 2a to a new one seen in 2b, an event that changes the validity of several nodes and edges.

presence of workspace changes [13,9] Since there is no extant code from either paper, we have implemented the algorithm from [9] ourselves, and tested our method against it both by comparing query times with a wide range of obstacles, and by comparing the runtimes of sequences of motion planning problems in a changing environment.

Similarly to [9], we also tested the runtime of motion planning queries computed by applying our method to a roadmap against single-query motion planning algorithms often used for non-static scenarios. Like [9], we use RRT [12] for these comparisons, and, for reasons later explained, chose to also include the LazyPRM algorithm [3] in our experiments.

Our experiments confirm that our data structure performs faster update operations than the only previous method, with average runtimes 10-40 percent faster depending on the size and shape of the modified obstacle (see Section 5.2 for details and Table 1 for results) and enables an augmented roadmap to solve motion planning queries faster than both single query algorithms and roadmaps utilizing the previous method by as much as  $\sim 60$  percent (see Section 5.3 for details and Tables 2 and 3 for results).

## 2 Related Work

In this section, we present the relevant body of work published on the problem and related subjects. We start by giving a brief review of some of the seminal work on sampling based motion planning, followed by a more in depth review of such work specifically designed for changing environments. We divide the latter part into two, LazyPRM adjacent work, and RRT adjacent work. Note that LazyPRM and RRT are the methods we use to demonstrate our contribution in Section 5.3.

## 2.1 Sampling-based motion planning

Sampling based motion planning (**SBMP**) is a motion planning approach in which  $C$ -space graphs are built using random sampling of nodes which are connected by edges computed by motion-planning primitives called *local planners*. This addition of randomness has been found effective in addressing the problem's intractability that expresses itself as a  $C$ -space of possibly exponential complexity in the size of the input.

Probabilistic Roadmaps (**PRM**), introduced by Kavraki *et al.* [11], are a family of **SBMP** algorithms that usually randomly sample node configurations, connect each configuration to some set of nearby nodes to form a graph (aka *roadmap*) containing representations of feasible paths. The roadmap is used to solve the motion planning problem by adding the start  $s$  and the goal  $t$  as new nodes of the graph and returning a graph  $(s, t)$ -path if one exists.

**PRMs** are usually used for the multi-query variant of the motion planning problem in which we are required to solve a set of motion planning problems for a single type of robot in a static workspace, as any change to either of these components results in changes to the implicit  $C$ -space and might render some of the graph's nodes and edges invalid. Many **PRM** variants exist and have been found to be applicable for a wide range of motion planning problems. See [16] and references therein.

The **RRT** algorithm introduced by LaValle [12] is a single query motion planning algorithm that expands a tree graph in the  $C$ -space by choosing a random point in the space and extending an edge towards that point from the nearest tree node. The **RRT** algorithm and its many variants, see [4] and references therein, are widely used both as stand-alone single query algorithms, and as a building block in many more complex methods, some of which we discuss below.

## 2.2 Planning in Modified Environments

The term “Modified environments” can be interpreted in two distinct ways. In this paper the changing nature of the environment is manifested in discrete changes to the location of obstacles, while other motion planning algorithms operate in the presence of a temporal dimension, meaning that certain obstacles have either known or estimated trajectories over time, and the algorithm must take these into account when computing the robot’s path. For the rest of this paper, this section excluded, we will use the adjective “modified” to mean the former.

**Dynamic Roadmaps** The papers most closely related to ours are by Leven and Hutchinson [13] and Kallmann and Mataric [9], where the latter built upon ideas from the former. Most notably, both papers approach the  $C$ -space - workspace relationship by partitioning the workspace using a fixed resolution grid, and maintaining lists of cell-node and cell-edge incidences. Despite the strong connection between the papers, the two focus on different aspects of the problem. The first paper ([13]) utilizes the similarity of lists of adjacent cells, where the best

definition of “adjacency” is one of the paper’s contributions, to create efficient representations of these incidence lists. The second ([9]) introduces a new update operation which relies on approximating the moved obstacle by its bounding box and focuses on the runtime when compared against RRT. Our contribution is much more closely aligned with that of [9], but where they used unions of uniform axis-aligned cubic grid cells in order to approximate the swept volumes, we use arbitrarily oriented and shaped *cigars* (see Section 3) to allow quick intersection checks and constant size space complexity per node/edge. Furthermore, where they used a uniform grid partition of workspace (even though both they and [13] mention the possibility of using an octree) we use a hierarchical, input sensitive decomposition. See Subsection 4.2.

**Lazy Evaluation** Bohlin and Kavraki’s LazyPRM [3] is a well known single query variant of the PRM algorithm. The lazy algorithm creates a roadmap without validating its edges, the part of PRM which usually requires the most runtime by an order of magnitude as a single edge can contain thousands of configurations that require validation. Some variants do not validate the nodes as well [2,3]. Given a motion planning query, the algorithm lazily connects the start and the goal to the roadmap and tries validating only the edges that lie on the shortest  $(s, t)$ -path in the roadmap. While this is not explicitly an algorithm meant for modified environments its “laziness” means that it can operate in modified environments (as we describe them) by simply ignoring all past information after each query.

LazyPRM has also inspired other algorithms meant specifically for changing environments. Jaillet and Simèon [7] gave a PRM based algorithm that computes a roadmap for the environment while considering only the static obstacles, and lazily evaluating a path by collision checking it only against dynamic obstacles that have moved in the vicinity of an  $(s, t)$ -path found in the roadmap. An important thing to notice is that if all of the obstacles are dynamic this algorithm degenerates to a variant of LazyPRM (as it does employ several other heuristics not found in [3]).

Hartmann *et al.* [6] describe a single query lazy motion planning algorithm for environments with *movable* objects that reuses computations by dividing validity checking efforts into several parts, and, given a query, validating the path by validating it against movable objects that have recently moved. Additionally, they give a PRM variant that, among other contributions, validates the robots’ collisions with itself and with static obstacles only when expanding the roadmap, and, much like [7], reuses that information when validating a path.

**Rapidly-exploring Random Tree (RRT) Algorithms** RRT is used in motion planning for changing environments due to its ability to quickly explore an unknown  $C$ -space. This property is extremely useful in these settings since a change to an obstacle’s position changes the landscape of the  $C$ -space and possibly invalidates some of a roadmap’s nodes and edges. An exploration process can then be employed in order to find a new path in a region where a path once existed [7].

Multipartite RRT [18] updates the validity of edges that have been obstructed by moved obstacles and stores the resulting disconnected subtrees in a cache. The root nodes of these subtrees are used as part of subsequent sampling. RT-RRT\* [15] grows an RRT\* [10] tree, an asymptotically optimal variant of RRT. When the obstacle moves, it rewrites the tree to not include any invalidated edges, and when the agent moves, the root is moved and the tree rewired around it to allow for multiple queries. In order to do this rewiring the paper searches adjacent cells with a simple grid-based spatial indexing.

Instead of taking a reactive planning approach, the workspace can be extended by a temporal dimension to incorporate known or predicted obstacle trajectories. SIPP [17] utilizes safe temporal intervals in a discretized space, where valid paths are found by using A\* to connect cells during safe intervals. ST-RRT\* [5] plans over continuous space with an added temporal dimension using random sampling. It uses a number of approaches to optimize sampling in both the spatial and temporal dimensions, such as conditional and weighted sampling. These planning methods are thus able to plan into the future around obstacle trajectories over time.

Note that the methods mentioned in the previous paragraph solve the single-query motion planning in a dynamic setting where obstacles move during the query phase. We therefore do not compare our data structure to these methods as they use extra computational resources for responding to online changes unlike single query algorithms for static environments.

### 3 Preliminaries

Let  $r$  be a robot,  $E = (B, O = \{o_i : i = 1, \dots, m\})$  be a 3D environment,  $\mathcal{C}_{space}$  be the implicit  $C$ -space defined by  $r$  and  $E$ , and  $G$  be a geometric graph in  $\mathcal{C}_{space}$ , i.e. a roadmap whose nodes and edges are points (configurations) and segments in  $\mathcal{C}_{space}$  respectively.

*Problem Definition* Given  $r, E, O$ , and  $G$  as an input, compute a dynamic graph  $H$  capable of performing 6DOF transformation updates of an object's location in workspace  $o_i \mapsto R \cdot o_i + T$ . At the end of the update operation all valid nodes and edges must be labeled as valid, and all infeasible nodes and edges must be labeled as invalid.

Let  $F_K : \mathcal{C}_{space} \rightarrow P(\mathbb{R}^3)$  be the *forward kinematics function* that, given a configuration  $c \in \mathcal{C}_{space}$ , returns the set of all points in  $\mathbb{R}^3$  that are occupied by  $r$  assuming the configuration  $c$ . With a slight abuse of notation we use  $F_K(C)$  for subsets  $C \subseteq \mathcal{C}_{space}$  to mean  $\bigcup_{c \in C} F_K(c)$ , and call the resulting 3D set the *swept volume* of  $C$ .

A node or an edge of  $G$  is *invalid* if its swept volume intersects any obstacle  $o_i$ , and otherwise it is *valid*. Note that this definition does not include robot self collision, kinodynamic constraints, and out-of-boundary constraints. This is suitable for our purposes as we only deal with movements of obstacles within  $B$  and their effect on  $G$ . This is not an issue because any of the aforementioned

conditions can be pre-computed once when computing  $G$  and have no further bearing on the problem. This simplification of the validity conditions allows us to reduce validity checking to 3D shape intersections which can be done very efficiently under some assumptions we consider to be reasonable. Our assumptions are as follows:

1.  $r$  can be approximated as a small set  $b_1^r, \dots, b_k^r$  of convex polyhedrons.
2. Every object  $o_i \in O$  can be approximated as a small set  $b_1^{o_i}, \dots, b_l^{o_i}$  of convex polyhedrons.
3. The approximations mentioned above are either given as part of the input or can be efficiently computed.

## 4 Method

As mentioned previously, in many high dimensional motion planning problems the relationship between the  $C$ -space and the workspace is neither easy to understand nor to compute. As such, we use rough approximations of the mapping between points and segments in the high-dimensional  $C$ -space to 3D volumes in workspace, and utilize common computational geometry tools in order to perform roadmap update operations. The shapes we are required to approximate are swept volumes of points and segments in  $\mathcal{C}_{space}$ , which, under our assumptions, are small sets of convex polyhedrons or linear motions (with rotations) of such polyhedrons. We approximate these polyhedrons using *cigars*.

A cigar, also called a capped cylinder, is the Minkowski sum  $s \oplus b$  of a segment and a ball, that is  $\bigcup_{p \in s} b(p)$  where  $b(p)$  is a translated copy of the ball  $b$  centered at  $p$ , and it is our “weapon of choice” for three main reasons; *a*) Cigars are very similar to ellipsoids which have been long known to provide decent approximations for high dimensional convex bodies [8], *b*) Linear motions of convex bodies tend to create long thin swept volumes which can be easily bounded by a cigar, and *c*) Distance and intersection computations involving cigars can be quickly approximated by viewing them as 3D segments with an associated radius.

In the following subsections, we describe the method by which we compute bounding cigars of swept volumes and create a data structure capable of storing a set of cigars and answering intersection queries of said set with simple shapes.

### 4.1 Swept Volume Approximation

Our assumptions immediately imply another assumption of many SBMP algorithms, which is that continuous motion can be sufficiently approximated by a discrete set of intermediate configurations. Given an edge  $(p, q) \in G$ , we first construct a point cloud  $P$  containing the vertices of  $F_K(c)$  for every intermediate  $c$  of  $(p, q)$ . We then use an algorithm for approximating the optimal volume oriented bounding box of a point cloud [1], and construct our cylinder from the resulted box. Note that rather than using the box itself as the 3D representation of the swept volume, we opted for using the smallest cigar containing the box for simpler and quicker intersection queries.

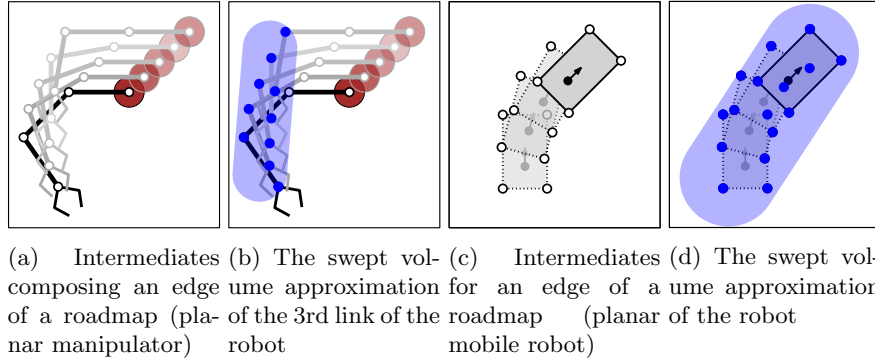


Fig. 3: In (a) we illustrate a set of configurations of a mobile manipulator with 2 translational DOFs and 3 angular joints composing an edge in some roadmap, and in (b) we see the point cloud and the cigar corresponding to the 3rd link of the robot. In (c) and (d) a similar process can be seen for a simple 3DOF planar robot.

## 4.2 Cigar Tree

We store the cigars in an axis-aligned bounding box tree (AABB tree), a data structure resembling a  $kD$ -tree in which every node is associated with an axis-aligned bounding box and the set of objects it contains, and the node’s children are constructed by splitting the bounding box perpendicularly to one of the axes and using some tie-breaker for objects intersecting the boxes of more than one child. Our implementation actually uses a ternary tree with all of the objects intersecting both sides stored in a separate child. Such geometric data structures may be problematic for certain inputs, for example a set of long segments with endpoints close to antipodal points of the scene’s bounding box cannot be easily separated along any of the 3 axes. This is, however, mostly irrelevant in our case due to the reasons described earlier in this section. Our data structure answers intersection queries in a straightforward AABB way. Given some query polyhedron  $Q$ , we start at the root and recurse on the children whose bounding box intersects  $Q$ , and, upon reaching a leaf of the tree, we check for intersections between the small (constant) number of cigars stored in that leaf and  $Q$  and append those that intersect to the output list.

Using the tools described above in conjunction with a simple data structure that stores for every obstacle  $o_i$  the list of edges and nodes it is currently invalidating we get a quick update operation described in Algorithm 1. The obstacle’s polyhedron or approximating polyhedron is passed as an argument to the tree’s intersection query resulting in a list of nodes and edges that need to be re-examined. This is followed by a re-examination of nodes and edges that were previously in collision with  $o_i$ .

---

**Algorithm 1:** Roadmap Update

---

```

input: Obstacle  $o$ , Transformation  $t$ 
1  $o.\text{UpdateLocation}(t)$ 
2  $\text{inv}C \leftarrow \text{Tree}.\text{GetIntersectingObjects}(o)$ 
3 for  $c \in \text{inv}C$  do
4   if  $CD(c,o) == \text{blocked}$  then
5      $c.\text{invalidate}()$                                 # Invalidating nodes and edges
6      $c.\text{intersectionList.add}(o)$ 
7   end
8 end
9  $\text{rev}C \leftarrow \text{Tree}.\text{GetIntersectedVolumes}(o)$ 
10 for  $c \in \text{rev}C$  do
11   if  $CD(c,o) == \text{free}$  then
12      $c.\text{intersectionList.remove}(o)$ 
13     if  $c.\text{intersectionList.IsEmpty}()$  then
14        $c.\text{validate}()$                                 # Re-validating nodes and edges
15     end
16   end
17 end

```

---

Some experiments not included in this paper actually show that the using the tree, as opposed to, say, a simple list of cigars, has very small effect on the runtime of graph update operations. This is true even though it is exponentially faster than linear scanning, and it is due to the runtime of the collision detection calls required to validate nodes and edges dominating the overall resulted runtime.

## 5 Experiments

With our experiments, we aim to validate our claims that 1) our approach results in faster update times for a dynamic roadmap in the presence of workspace changes, and 2) this faster update time of the dynamic roadmap enables faster motion planning in multi-query scenarios than single query algorithms traditionally used for non-static scenarios.

### 5.1 Experimental Setup and Implementation Details

In order to demonstrate our claims we run two sets of experiments.

In the first set, we directly measure the improvement in the roadmap update time against a brute-force benchmark and against an implementation of the method described in [9], which, as mentioned in Section 2, is the only method for  $C$ -space graph updates for modified environments we were able to find in the literature. We refer to this algorithm as the *grid method*. Note that we have implemented the grid method ourselves based on the paper.

In the second set, we use our data structure as part of a multi-query motion planning algorithm and compare its performance against the grid method, RRT,

and **LazyPRM**. These experiments capture the applicability of our data structure in lieu of the results showcased by the first experiment, and demonstrates its ability to allow fast pathfinding operations in  $C$ -space in a modified setting for both mobile robots and manipulators. The grid method was previously only compared to RRT, but we have decided to compare our method against **LazyPRM** as well since **LazyPRM** is not only a fast single query **SBMP** algorithm, but one that can take an unvalidated roadmap as an input which may considerably improve its performance, e.g., when the provided roadmap contains a valid path.

Our method and the grid method only maintain and update the validities of the roadmap nodes and edges when obstacles are moved, and so in order to fairly compare the runtime of motion planning queries against single-query methods we measure the roadmap update time in addition to the time needed for the roadmap to answer the motion planning query. We stress that our method does not assist in pathfinding or the creation of better roadmaps, only adjusts such graphs to allow them to operate on modified environments. For this reason we use an input graph guaranteed to contain a solution, and the same graph is provided to all methods for a fair comparison. This choice of roadmap demonstrates that, given an appropriate graph to build upon, our method provides a better solution for multiple queries in a modified environment than using the grid method or single query algorithms.

**SPITE Implementation** Our method uses two computational geometry components for its purpose, one for approximating 3D volumes with cigars, and one for storing the cigars and answering intersection queries. Since the runtimes related to the cigar tree operations have almost no impact on the overall runtime, as they are smaller than those required for full collision checks by orders of magnitude, we did not bother to optimize them.

The approach for computing the cigars employs an algorithm for constructing an approximately optimal oriented bounding box [1] for which we have chosen the approximation factor 0.1.

We determine the set of cigars intersecting an obstacle, and by extension, the set of nodes and edges possibly invalidated by a modification to the workspace, by querying the cigar tree with the obstacle's axis aligned bounding box. The set of previously invalid nodes and edges that need to be re-checked is compiled by storing an incidence list of obstacles and nodes/edges, and all fine-grained collision checking is done by the collision detection function.

**Grid Method Implementation** The grid method partitions the workspace into uniform cubes of some pre-determined side length and computes for each cell the set of nodes corresponding to configurations intersecting that cell and edges corresponding to movements whose swept volume intersects it. This can be viewed as approximating the 3D volumes occupied by robot configurations and movements by a subset of axis-aligned uniform size cubes. Given an update in an obstacle's position the method computes the axis-aligned bounding box of the obstacle in its new configuration and reports all of the nodes and edges listed in

workspace cells with non-empty intersection with the obstacle’s bounding box. The validity of these nodes and edges is then checked using the collision detection function.

This method offers a trade-off between pre-processing time and update time. The pre-processing phase can be somewhat expensive if the chosen cell size is small due to the well known exponential increase in complexity incurred by grid data structures. On the other hand if the cells are large that will result in many unnecessary and expensive collision detection calls that will be performed as obstacles intersect the grid cell more often during updates, and each such grid cell is associated with a prohibitively long list of affected nodes and edges.

Because of this we report at least two instances of the grid method for every experiment in order to demonstrate that the discrepancy between SPITE and the grid method is not an artifact of the parameters used.

**LazyPRM Implementation** The first single query method we compare against is LazyPRM [3]. We test LazyPRM by giving it the same roadmap used by our data structure as an argument. LazyPRM connects the start and goal configurations to the roadmap graph, finds a path in the graph, validates its vertices, and only validates its edges if all previous steps were successful. The path validation process uses hierarchical validation, meaning, first attempts to validate the path at a coarse resolution (one in every 27 intermediates of an edge), and only if the entire path is valid at that resolution moves forward to a finer resolution (one in 16) and finally completely validates the path.

Since this implementation of LazyPRM first validates the vertices of a path before launching an expensive edge validation, we ensure that at least in the mobile robot experiment the validity of the nodes along a path are a perfect indication of the validity of its edges, thus maximizing the efficiency of LazyPRM as much as possible. Since the roadmaps used for the manipulators were randomly created we did not guarantee this property in those experiments.

**RRT Implementation** The second method we compare against is RRT [12]. Our implementation is standard. We use minimum and maximum extension distances to be 0.1 and 4.0 respectively. Out of all the methods we use in this experiment RRT is the only one which does not use an initial roadmap since it performs pathfinding directly in  $C$ -space. All other methods use a roadmap as an argument and perform path finding only on that roadmap.

*General implementation details* All experiments were run on a desktop computer with an Intel Core i7-3770 at 3.40GHz, 16 GB of RAM. The Parasol Planning Library (PPL) implementations were used for all SBMP functions and algorithms.

## 5.2 Dynamic Roadmap Updates

In the first experiment, we test our graph update method against the grid method and a brute-force method. Our method and the grid method compute a set

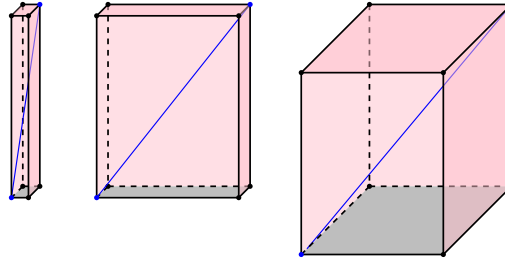


Fig. 4: Different orientations of similar line segment obstacles (in blue) and their corresponding axis-aligned bounding boxes.

of nodes and edges and then validate only that set using fine-grained collision detection. The brute-force method re-validates every node and edge in the graph with no regard to the workspace changes that took place. Note that all methods use the same collision detection algorithm which only performs collision detection against the subset of obstacles whose position has changed.

The experiment environment is a cube  $[-16, 16]^3$  with a single axis-aligned rectangular prism obstacle. The robot is a simple 6DOF rectangular prism. Experiments are run with nine different shapes and sizes of the rectangular prism obstacle, which results in different queries to the grid data structure and the cigar tree. We use rectangular obstacles of varying sizes and shapes because it mimics the bounding boxes of differently shaped obstacles. Both data structures, i.e. the cigar-tree and the grid, use the axis-aligned bounding box of the obstacle when computing the intersected regions (tree leaves and grid cells respectively). For example, the update operation required for an arbitrarily oriented long and thin obstacle  $o$  will result in a data structure query which could be a long and thin axis-aligned box if  $o$ 's orientation is close to parallel to one of the axes and perpendicular to all other axes, but could also be a “slice” of the environment or even a large cube if the orientation is diagonal in some or all of the dimensions. See Figure 4 for a visualization of this.

Three sets of experiments are performed with cube-shaped obstacles of side lengths 2, 5, and 20, and six sets experiments are performed with prisms of dimensions  $[20 \times 20 \times 1]$ ,  $[20 \times 1 \times 1]$ ,  $[20 \times 20 \times 2]$ ,  $[20 \times 2 \times 2]$ ,  $[20 \times 5 \times 5]$ , and  $[20 \times 20 \times 5]$ .

We created a roadmap with 1000 nodes and  $\sim$ 5000 edges using a uniformly sampling PRM algorithm where each node is connected to its 6 nearest neighbors. Then we constructed our data structures with the roadmap as input. Both our data structure and the grid method have a pre-processing phase where the graph nodes and edges are mapped to workspace objects (cigars and grid cells respectively) and checked for validity. Notice the time required for this pre-processing step is not included in the average comparison time, but is included as part of the reported results. We perform 100 random location changes for each obstacle size, each followed by a roadmap update operation with the change to the obsta-

obstacle	SPITE(ms)	Grid_1(ms)	Grid_2(ms)	Grid_4(ms)	Grid_8(ms)	BF
$1 \times 1 \times 1$	5.3	8.9	15.8	36.0	116.3	$\sim 4$ sec
$1 \times 1 \times 1$	50.3	67.0	93.9	149.8	296.9	
$20 \times 2 \times 2$	39.7	57.2	85.2	152.6	343.1	
$5 \times 5 \times 5$	58.0	70.7	95.7	153.4	301.4	
$20 \times 20 \times 1$	212.2	246.9	314.3	453.0	718.8	
$20 \times 5 \times 5$	136.7	166.1	212.7	300.9	478.3	
$20 \times 20 \times 2$	292.1	337.9	417.5	577.8	872.9	
$20 \times 20 \times 5$	422.4	465.6	538.7	708.6	974.9	
$20 \times 20 \times 20$	610.7	778.9	773.8	924.4	1126.8	
Pre-processing time	2 min	29 hrs	4 hrs	34 min	4 min	-

Table 1: Comparison of dynamic roadmap updates using SPITE and grid with different cell sizes. BF stands for brute force, and Grid\_i refers to the grid method with cells of side length i. All results for which a time unit is not disclosed are in milliseconds. Best result in every row is highlighted green, the last row has lighter green for best pre-processing time out of methods with such a runtime component.

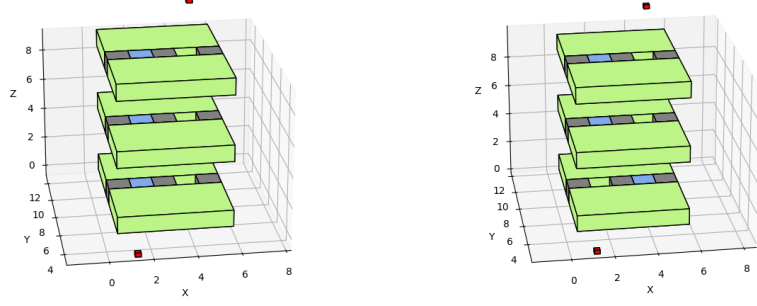
cle location as an input. We measure and compare the time required to perform an update.

The results are shown in Table 1.

### 5.3 Motion Planning Queries

A natural way of using a data structure such as ours is using it to perform obstacle update operations on a roadmap when obstacles change position, and use that roadmap to answer motion planning queries as they are given. Another way to handle environment changes between motion planning queries is to not store any C-space information and solve motion planning queries using a single query algorithm. In this set of experiments, we evaluate this latter option against our data structure and the grid method by comparing the run-time of single query algorithms against the combined runtime of a data structure update method and a motion planning query using the roadmap.

**Mobile Robot Experiment** We run the experiment on the environment shown in Figure 5, which contains three walls, each with two possible locations of a narrow passage. The experiment consists of 1000 iterations, in each of which we change the location of the passage in each wall with probability 1/2. Our robot is a small translational cube of side-length 1/4th that of the passage. Note that using a 6DOF robot would increase the search space of RRT while not changing anything about the runtime of the other methods which use a fixed size roadmap. For each iteration, we generate random start and goal queries in opposite sides



(a) The starting position of every obstacle in the environment  
(b) A random movement of the blue obstacles. Only the lowest obstacle switched to other position.

Fig. 5: An illustration of the environment used for the experiments described in Section 5.3. Two configurations of the translational cube robot are seen in red. In every Iteration of the experiment each of the blue obstacles changed its position with probability 1/2. Note that the bounding box is not illustrated for the sake of clarity.

Query Method	Update(s)	Query (s)	Total	Pre-processing (min)
PRM + SPITE	0.13	0.12	0.25	0.95
PRM + Grid_1	0.14	0.15	0.28	40.3
PRM + Grid_2	0.39	0.14	0.52	7.6
LazyPRM	-	1.84	1.84	-
RRT	-	10.68	10.68	-

Table 2: Comparison of graph-based motion planning algorithms augmented for modified environments and single-query motion planning algorithms in a mobile robot scenario. Grid\_i indicates the grid method with cells of side length  $i$ , and the best results are shown in green. Note that the best pre-processing time out of the methods with a pre-processing phase is highlighted in lighter green.

of the environment, requiring each query to find a path through all three narrow passages. All methods except RRT are provided the same  $C$ -space roadmap. This roadmap is an induced subgraph of the 3D graph with resolution (i.e. edge length 1/4) on  $\sim 3400$  nodes, and is guaranteed to contain a valid path through all three walls regardless of obstacle locations and, therefore, from any sampled start to any sampled goal configurations.

The results of the experiment are presented in Table 2.

**Manipulator Experiment** For this experiment we use a simulation of a 5DOF UR5e in a shelf environment shown in Figure 1. The two-story shelf contains two obstacles, a spray can and a box which are located at the center of either the

Query Method	Update(s)	Query (s)	Total	Pre-processing (min)
PRM + SPITE	0.199	0.028	0.227	27.6
PRM + Grid_0.5	0.773	0.029	0.802	89.9
PRM + Grid_1	9.310	0.165	9.475	12.3
LazyPRM	-	0.349	0.349	-
RRT	-	*0.016	*0.016	-

Table 3: Comparison of graph-based motion planning algorithms augmented for modified environments and single-query motion planning algorithms for a UR5e in a shelf environment. Grid\_i indicates the grid method with cells of side length  $i$  meters, and the best results are shown in green. Note that the best pre-processing time out of the methods with a pre-processing phase is highlighted in lighter green, and runtimes hiding a success rate of only 53 percent are highlighted red.

top or bottom shelf with probability  $1/2$  each. The simulated environment size is  $6 \times 6 \times 4$  meters, though out of these the volume reachable by the robot is much smaller, and the physical setup is contained in a  $2 \times 2 \times 1$  meter region. All algorithms except for RRT were provided with a roadmap containing 1000 nodes that was guaranteed to contain a path regardless of the obstacles’ positions. We performed 100 iterations using a single start  $s$  and goal  $t$  pair, where the robot’s endeffector is located at the back right corner of the upper shelf in configuration  $s$ , and in the back left corner in configuration  $t$ . In this experiment we have capped the runtime of RRT at 60 seconds.

The paths produced in this experiment specifically for the instances where both objects were placed in the same shelf were validated using the physical setup shown in Figure 1 and in the videos provided as supplemental material.

The results of the experiment are presented in Table 3. Notice that RRT had a success rate of 53 percent.

#### 5.4 Discussion

The first experiment, described in Section 5.2, demonstrates that for many “reasonably” shaped obstacles SPITE outperforms the grid method in update times while requiring a fraction of the preprocessing time. As the size of the obstacle increases to a diameter more than half that of the environment we see in Table 1 a clear increase in update times due to the sheer number of nodes and edges which are invalidated and re-validated at every iteration.

The most glaring detail about this experiment is the exponential increase in pre-processing time that plagues the grid method, with a factor of close to the expected  $2^d$  factor in the runtime with every refinement of the grid that is translated to diminishing returns in update performance, resulting in a 29 hours pre-processing time required to construct a data structure with  $32^3$  cells in order to compete with our method. This is by far the largest environment of all of the experiments and thus the one where this effect can be most easily seen.

---

\*53% success rate

The table also shows us that while there is no clear trend in the relative difference between update times of SPITE and the grid method, there is an increase in absolute difference as obstacles increase in size. Note that this result carries over to the case of multiple updated obstacles as all methods will sequentially perform the updates for each moved obstacle.

The second and third experiments, described in Section 5.3, showcase the contribution of these faster updates when performing motion planning queries.

In the mobile robot experiment, described in the first part of Section 5.3 and summarized in Table 2, we see that unlike the dynamic roadmaps, RRT and LazyPRM are both affected by the distance between the start and goal configurations, as it directly increases the number of collision checks they need to perform, and all of the methods that utilize a roadmap benefit greatly from circumventing the need to perform pathfinding in  $C$ -space.

The small modifications which are due to the small obstacles and a small and fat robot result in smaller scale updates and thus a lead to mild absolute update time differences.

In the last experiment, described in the second part of Section 5.3 and summarized in Table 3, we see that as the robot becomes more complicated, e.g. composed of more bodies, some of which are not fat, and as the obstacles occupy more of the reachable volume required to perform the motion planning task, the runtime difference is strongly pronounced with our method requiring  $\sim 60$  percent less runtime than the grid method while requiring significantly less pre-processing time. Notice that in this more complicated scenario even a very coarse grid requires a substantial preprocessing time. We believe that the extremely sharp decrease in query time is a result of large fractions of the edges in the roadmap intersecting a few grid cells with side length 1.

LazyPRM does indeed perform much better due to the relatively short distances, a fact which is not enough to compensate for the difficulty of the pathfinding task when the top shelf contains one of the objects thus causing RRT to not be able to complete the task within the allotted 60 seconds.

## 6 Conclusion

In this paper, we introduced the SPITE supplementary method for dynamic roadmaps and an approach to 3D volume approximation with a matching hierarchical collision checking method for nodes and edges in  $C$ -space graphs. We found our method outperforms the only previously known method in both update and pre-processing times, and, when used in the context of motion planning queries can lead to faster motion planning queries for mobile robots and manipulators in modified environments than single-query algorithms.

For future work, we plan to focus on the 3D swept volume approximation, adding lower-bound approximations and using oriented bounding boxes instead of cigars, and add lazy planning heuristics to our method.

## References

1. Gill Barequet and Sariel Har-Peled. Efficiently approximating the minimum-volume bounding box of a point set in three dimensions. *J. Algorithms*, 38(1):91–109, 2001.
2. R. Bohlin and L. E. Kavraki. A randomized algorithm for robot path planning based on lazy evaluation. In P. Pardalos, S. Rajasekaran, and J. Rolim, editors, *Handbook on Randomized Computing*, pages 221–249. Kluwer Academic Publishers, 2001.
3. Robert Bohlin and Lydia E. Kavraki. Path planning using lazy prm. In *Proc. IEEE Int. Conf. Robot. Autom. (ICRA)*, April 2000.
4. Mohamed Elbanhawi and Milan Simic. Sampling-based robot motion planning: A review. *IEEE Access*, 2:56–77, 2014.
5. Francesco Grothe, Valentin N Hartmann, Andreas Orthey, and Marc Toussaint. St-rrt\*: Asymptotically-optimal bidirectional motion planning through space-time. In *2022 International Conference on Robotics and Automation (ICRA)*, pages 3314–3320. IEEE, 2022.
6. Valentin N. Hartmann, Joaquim Ortiz de Haro, and Marc Toussaint. Efficient path planning in manipulation planning problems by actively reusing validation effort. In *IROS*, pages 2822–2829, 2023.
7. Leonard Jaillet and Thierry Siméon. A prm-based motion planner for dynamically changing environments. In *2004 IEEE/RSJ International Conference on Intelligent Robots and Systems, Sendai, Japan, September 28 - October 2, 2004*, pages 1606–1611. IEEE, 2004.
8. Fritz John. Extremum problems with inequalities as subsidiary conditions. *Traces and emergence of nonlinear programming*, pages 197–215, 2014.
9. M. Kallman and M. Mataric. Motion planning using dynamic roadmaps. In *Proc. IEEE Int. Conf. Robot. Autom. (ICRA)*, volume 5, pages 4399–4404, April 2004.
10. S. Karaman and E. Frazzoli. Incremental sampling-based algorithms for optimal motion planning. In *Proceedings of Robotics: Science and Systems*, Zaragoza, Spain, June 2010.
11. L. E. Kavraki, P. Švestka, J. C. Latombe, and M. H. Overmars. Probabilistic roadmaps for path planning in high-dimensional configuration spaces. *IEEE Trans. Robot. Automat.*, 12(4):566–580, August 1996.
12. Steven M. LaValle. Rapidly-exploring random trees: A new tool for path planning. Technical report, Iowa State University, 1998.
13. Peter Leven and Seth Hutchinson. A framework for real-time path planning in changing environments. *Int. J. Robotics Res.*, 21(12):999–1030, 2002.
14. T. Lozano-Pérez and M. A. Wesley. An algorithm for planning collision-free paths among polyhedral obstacles. *Communications of the ACM*, 22(10):560–570, October 1979.
15. Kourosh Naderi, Joose Rajamäki, and Perttu Hämäläinen. Rt-rrt\* a real-time path planning algorithm based on rrt. In *Proceedings of the 8th ACM SIGGRAPH Conference on Motion in Games*, pages 113–118, 2015.
16. Andreas Orthey, Constantinos Chamzas, and Lydia E. Kavraki. Sampling-based motion planning: A comparative review. *CoRR*, abs/2309.13119, 2023.
17. Mike Phillips and Maxim Likhachev. Sipp: Safe interval path planning for dynamic environments. In *2011 IEEE International Conference on Robotics and Automation*, pages 5628–5635. IEEE, 2011.

18. M. Zucker, J. Kuffner, and M. Branicky. Multipartite rrt for rapid replanning in dynamic environments. In *Proc. IEEE Int. Conf. Robot. Autom. (ICRA)*, pages 1603–1609, April 2007.